Acoust. Sci. & Tech. **25**, 1 (2004)

ACOUSTICAL LETTER

High-resolution broadband beamforming and detection methods with real data

Shefeng Yan and Yuanliang Ma

Institute of Acoustic Engineering, Northwestern Polytechnical University, Xi'an, P.R. China

(*Received 29 April 2003, Accepted for publication 12 June 2003*)

Keywords: Passive sonar, High-resolution, MVDR Beamforming, SPED, Real data

PACS number: 43.30.−k [DOI: 10.1250/ast.25.73]

1. Introduction

As the acoustic noise sources become quieter and quieter, detection and localization of the acoustic source become more and more difficult. The noise sources are often many dB quieter than the acoustic noise floor and the source noise field is unknown in that the signal strength and spectra of the source are unknown. In addition, the target is often submerged in multiple noise sources. On the other hand, spatial discrimination capability (the ability to separate two plane-wave signals whose arrival angles are closely spaced) depends on the size of the spatial aperture. We are constrained by the geometric and performance limitations of the available acoustic array. It is necessary to find good beamformer and broadband detection methods with high resolution to detect and track low signal-to-noise ratio (SNR) multiple targets.

High-resolution adaptive beamforming techniques for underwater applications have been extensively studied for past several decades [1]. However, not many applications have been reported in the public domain. Furthermore, most of the works reported in the literatures were for narrowband array processing. Although broadband beamforming implement procedure has been reported [2–4], most of them are for conventional beamforming.

The goals of broadband detection are to condense the information contained in an array's beamformer output and aid operators in detecting acoustic targets. Conventional Energy Detection (CED) is often implemented as optimal signal detection in uncorrelated noise fields. It provides good detection ability with uncluttered targets and the best theoretical Minimum Detectable Level (MDL) than all other energy detectors. However, it has wide blurry traces for loud targets and poor bearing resolution. It also has impaired detection ability in real world (cluttered) noise environments.

Subband Energy Detection is another new class of important broadband processing method that provides improved performance to sonar systems [5]. One of them is called Subband Peak Energy Detection (SPED). SPED can provides thinner target traces, improved bearing resolution, and better detection advantage in real world (cluttered) acoustic environments. The author's group have given the principle and simulation results for SPED earlier in reference [6], results on real data will be presented in the paper.

2. High resolution beamforming

A beamformer is a processor used in conjunction with an array of sensors that collects spatial samples of propagating wave fields to provide a versatile form of spatial filtering. It is employed to resolve or separate signals coming to the sensor array from different directions. By providing a specified gain at the looking direction and attenuation for other directions, a beamformer enhances the desired signals and in the same time suppresses the undesired interferences.

Beamformers can be classified as either data independent or statistically optimum depending on how the weights are chosen. The weights in a statistically optimum beamformer are chosen based on the statistics of the array data to "optimize" the array response. In general, the statistics optimum beamformer attempt to maximize the signal to noise ratio at the beamformer output. Among them the Minimum Variance Distortionless Response (MVDR) beamformer shows significant advantages. MVDR maintains a constraint of beam response at a look direction being unit while minimizes the total power output of the weighted sum of the received sensor data. The minimization suppresses all the discrete sources in spatial domain except the signal at the look direction, and therefore results in maximum output signal to noise ratio and high-resolution.

The beamforming procedure changes with the bandwidth of the signals to be received: the signal bandwidth is roughly divided into narrowband and broadband, depending on whether the signal can be adequately characterized by a single frequency (i.e., components with bandwidths small compared to their center frequency).

If the signal is narrowband with central frequency f, the narrowband beamformer output is

$$b(f,t) = \boldsymbol{w}^{\mathrm{H}}(f)\boldsymbol{x}(t) \tag{1}$$

where $\boldsymbol{w}(f) = [\boldsymbol{w}_1(f), \boldsymbol{w}_2(f), \ldots, \boldsymbol{w}_M(f)]^{\mathrm{T}}$ stands for the weight vector at frequency f, $\boldsymbol{x}(t) = [x_1(t), x_2(t), \ldots, x_M(t)]^{\mathrm{T}}$ the observed narrowband data vector whose central frequency is f, M the number of elements, superscript H denotes transpose conjugate of matrix.

The weight vector for MVDR beamformer can be obtained as

$$\boldsymbol{w} = \frac{\boldsymbol{R}_x^{-1}\boldsymbol{d}(\theta, f)}{\boldsymbol{d}(\theta, f)^{\mathrm{H}}\boldsymbol{R}_x^{-1}\boldsymbol{d}(\theta, f)} \tag{2}$$

where $\boldsymbol{R}_x = E\lfloor \boldsymbol{X}(t)\boldsymbol{X}^{\mathrm{H}}(t) \rfloor$ is the $M \times M$ array output covariance matrix, $\boldsymbol{d}(\theta, f)$ the steering vector.

The output power of the beamformer is

$$P(\theta, f) = \frac{1}{d(\theta, f)^{\mathrm{H}}\boldsymbol{R}_x^{-1}\boldsymbol{d}(\theta, f)} \tag{3}$$

The estimate of sample covariance matrix is obtained by:

$$\hat{\boldsymbol{R}}_x = \frac{1}{K}\sum_{k=0}^{K-1} \boldsymbol{x}(k)\boldsymbol{x}^{\mathrm{H}}(k) \tag{4}$$

Translate narrowband signal $\boldsymbol{x}$ from the sensor array to its baseband through complex demodulation, get

$$\boldsymbol{y}(n) = \boldsymbol{x}(n)e^{-j2\pi nf/f_s} \quad \text{or} \quad \boldsymbol{x}(n) = \boldsymbol{y}(n)e^{j2\pi nf/f_s} \tag{5}$$

where f_s is sampling frequency. Then

$$\hat{\boldsymbol{R}}_x = \frac{1}{K}\sum_{k=0}^{K-1} y(k)e^{j2\pi nf/f_s}\boldsymbol{y}^{\mathrm{H}}(k)e^{-j2\pi nf/f_s} = \frac{1}{K}\sum_{k=0}^{K-1} \boldsymbol{y}(k)\boldsymbol{y}^{\mathrm{H}}(k) \tag{6}$$

that is, we can obtain the sample covariance matrix through the baseband complex signal of the narrowband signal, so do the weight vector and beamformer output power.

If the signal $\boldsymbol{x}$ received from a sensor array is broadband, it can be subdivided into subbands. Each subband is then translated to baseband through complex demodulation. Subsequently, pass a FIR Low-Pass Filter (LPF) h_N with a length of N. The band shifting and filtering are performed on consecutive subbands. For the sampled sequence, $x_m(n)$, derived from the mth element, the output signal of the subband filter, $y_m(n)$, can be expressed as

$$y_m(l) = \sum_{n=l-N}^{l-1} h_N(l-n)x_m(n)e^{-j2\pi nf/f_s} \tag{7}$$

Since its bandwidth is greatly reduced, the baseband signal can be decimated to improve the computational efficiency. For decimation factor N, let $l = n'N$ and $f = f_s \cdot (k/N)$, the output signal for input raw data $x_m(n)$ $(n = 0, 2, \ldots, N-1)$ is

$$y_m{}'(n') = \sum_{n=(k-1)N}^{kN-1} h_N(kN-n)x_m(n)e^{-j2\pi nf/N} \tag{8}$$

the demodulation and summation operations in the above equation has the same form as the Discrete Fourier Transform (DFT) and thus can be implemented by FFT.

The broadband beamforming for MVDR can be implemented as follows. The broadband signals received from array sensors are subdivided into many segments with a length of N. The data are then transformed by Short Time Fourier Transform (STFT) proceeded by the data windowing h_N. Subsequently, the data vectors coming from STFT are used to estimate covariance matrix $\hat{\boldsymbol{R}}_x$ and MVDR weight vector, then beamformed for all subbands data and finally energy detection.

MVDR beamforming outperforms its conventional counterpart. The MVDR beamforming results for real data has been presented reference [7] and will not discussed in this paper.

3. High resolution detection

In a multibeam sonar system, a CED broadband processor block diagram is given in Fig. 1. The outputs of beamformer for every frequency bin is further processed using a Square-Law-Detector (SLD) function. After that, the outputs are averaged over time (Time Average, TA) then normalized [8–10] and weighted usually by Eckart weighting. To match

3. HIGH RESOLUTION DETECTION

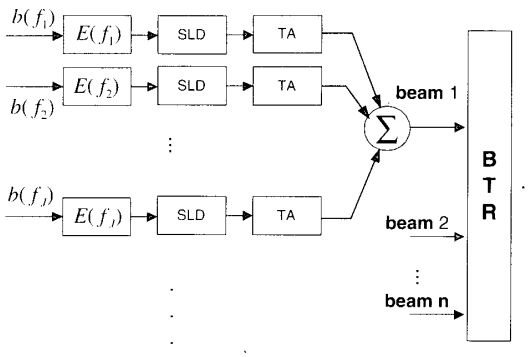

Fig. 1 Block diagram of CED.

between the observation time and the signal stationarity, a number of different averaging time are provided. The normalization is accomplished in the frequency domain separately at each beam. The Eckart weighting factor is obtained based on the shape of signal power spectrum and noise spectrum. Subsequently, sum the output data over frequencies for each single azimuth bin (single beamformer) to provide a bin energy estimate. Finally, broadband detection in a multibeam sonar system is accomplished by viewing the BTR data on a "waterfall" display. A horizontal line of data consists of outputs from the beams, and it is available for display each time a sequence of outputs. From the BTR "waterfall" diagram, we can detect the source in a particular bearing. Multiple targets are distinguished by their separation in bearing on the display.

SPED is an important broadband processing method that provides improved performance to sonar systems whose block diagram is given in Fig. 2. The data from the beamformer for each frequency bin is just the same with CED while the energy detection algorithm is different.

Acoustic energy from a target signal or random noise generates "peaks" and "valleys" in both time and frequency. Looking at the frequency spectrum of a low SNR target, the background noise occasionally drops below the level of the

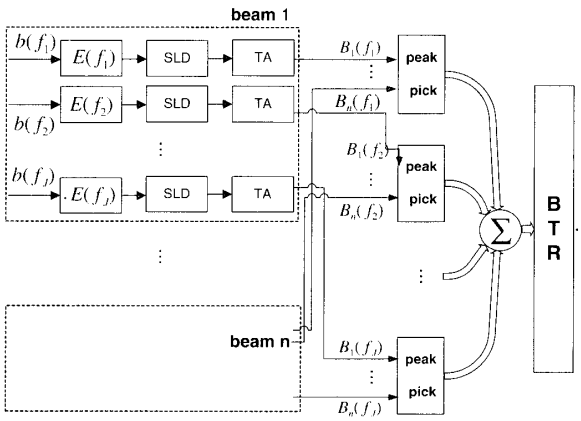

Fig. 2 Block diagram of SPED.

target signal. When this happens, there is a peak due to the target signal. Now, looking at one frequency bin of the beam noise versus azimuth spectrum (multibeam output) there may be several peaks due to the signal but still many more due to noise.

Instead of summing the energy in a single azimuth bin for all frequency bin, SPED utilizes only the "peak" information to estimate the detection probability. It looks for peaks (peak picking) in the azimuth spectrum for every single frequency bin. Ultimately, a weighted sum of the 'energy' values of the peaks is calculated over all frequency bins for each time scan and azimuth bin, then display in a BTR "waterfall" diagram.

Peaks due to the directional source will occur in the same azimuth bin for each frequency bin. These peaks have spatial coherence and can add "constructively" when summed over the entire range of frequency bins. On the other hand, peaks due to random noise will occur in different azimuth bin for different frequency bin. They will not exhibit spatial coherence and will not add "constructively." That makes low SNR targets can be detected.

In CED, the inherent beam width makes display stronger in the beam near the source azimuth than other beams. This makes CDE wide blurry traces for loud targets and poor bearing resolution. In SPED, however, the "peak-picking" effectively reduces the bearing ambiguity between adjacent beams and provides sharper, more clearly defined target traces thus improved spatial resolution of the acoustic environment.

4. Results on simulated and real data

Suppose two signals arrive from 106° and 126° with SNR=−18 dB at a 24-element circular hydrophone array. The beams output powers (with 5 second of time average) of MVDR beamformer for 23 frequency bins (center at 704 Hz, 768 Hz, ···, 2,112 Hz) and 72 azimuth bins (0°, 5°, ···, 355°) are computed and display in Fig. 3 as FRAZ (frequency v.s. azimuth) diagram. The corresponding peak energy is shown in Fig. 4. Sum the output energy over frequencies for each single azimuth bin to get azimuth energy spectrum. Beam azimuth energy values for 72 steering angles are interpolated to 360 for display, which is shown in Fig. 5. The corresponding azimuth peak energy spectrum is shown in Fig. 6. It can be seen from Fig. 5 and Fig. 6 that SPED has higher bearing resolution than CDE.

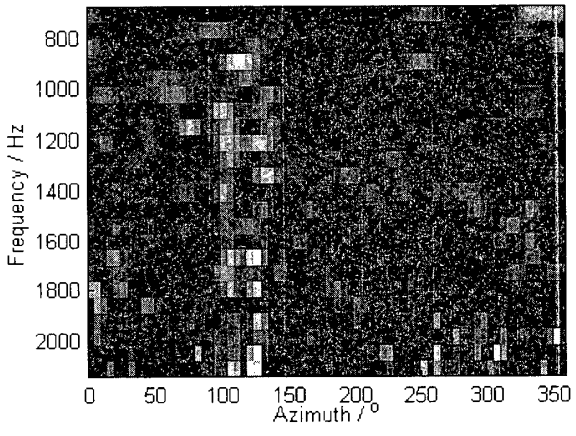

Fig. 3 Energy in FRAZ.

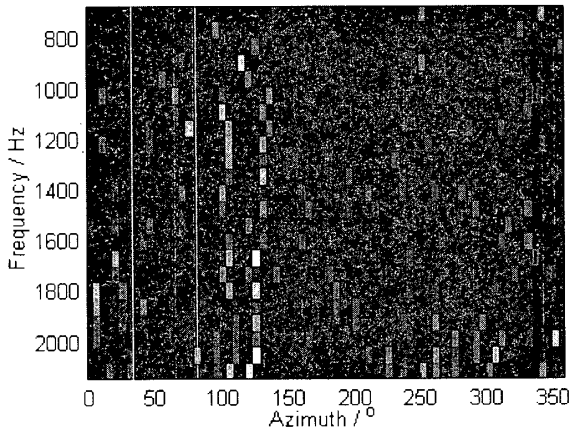

Fig. 4 Peak energy in FRAZ.

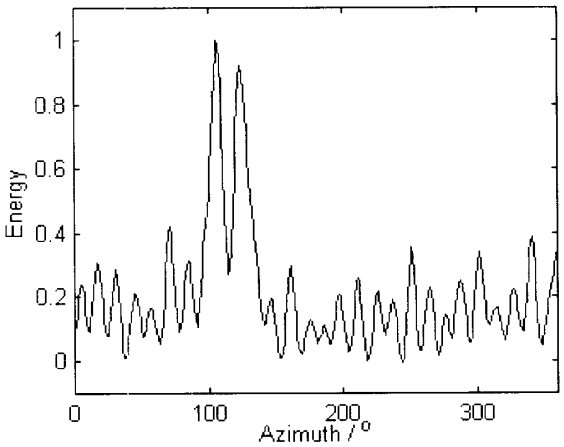

Fig. 5 Azimuth energy spectrum.

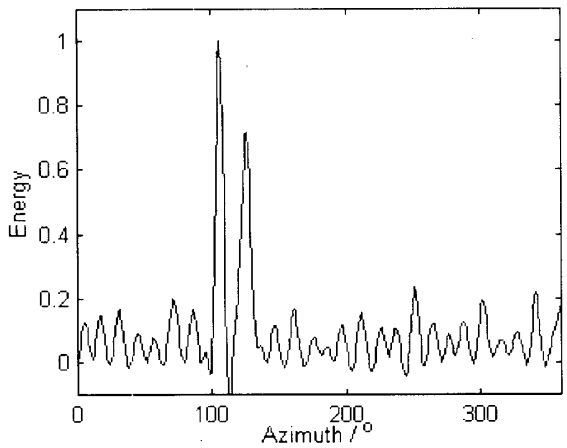

Fig. 6 Azimuth peak energy spectrum.

In our experiment, the experimental data was recorded using a 24-element circular hydrophone array. The sampling frequency for the real data was 8,192 Hz. Using a 128 point STFT to get 128 subbands and 23 subbands (center at 704 Hz, 768 Hz, ···, 2,112 Hz) of them are used. 180 beams in 0 ~ 360° azimuth angle are formed for each of the 23

subbands, beam output energy is then computed. Energy sum and peak energy sum of 5 second data are employed respectively by combining the 23 subband results. CED output energy values and SPED output energy values for 180 azimuth angles v.s. time are shown in Fig. 7 and Fig. 8 respectively.

Comparing Fig. 8 to Fig. 7, as we have expected, the SPED shows far better resolution than the conventional one. Tracks of noise sources are thin and bright in the SPED result. Therefore, the SPED detection and tracking capability for weak sources with the presence of strong sources are far enhanced.

5. Conclusion

The broadband high-resolution beamforming and high-resolution detection methods are presented in this paper. The broadband beamforming procedure is discussed for MVDR. SPED is also introduced as a high-resolution detection method. The results on simulation and real data show that SPED can obtain higher bearing resolution and detection ability compared to CED. The presented approaches have also been shown to be simple and practical as verified by an experimental data set collected in shallow water.

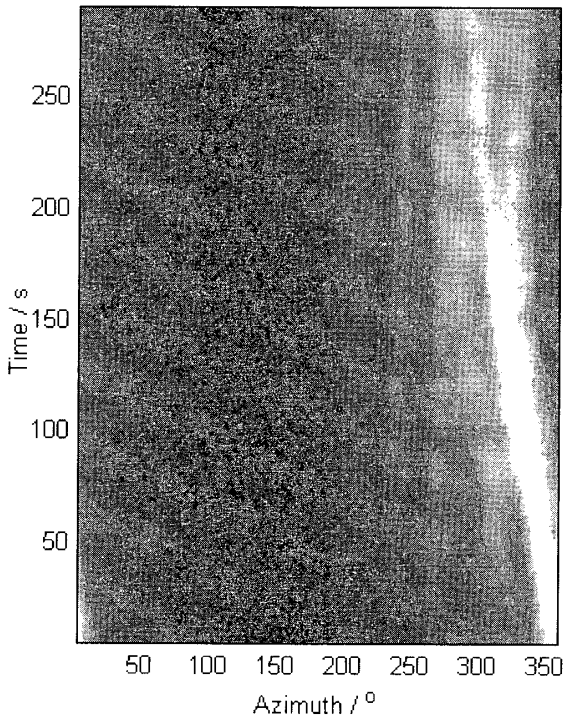

Fig. 7 BTR from CED.

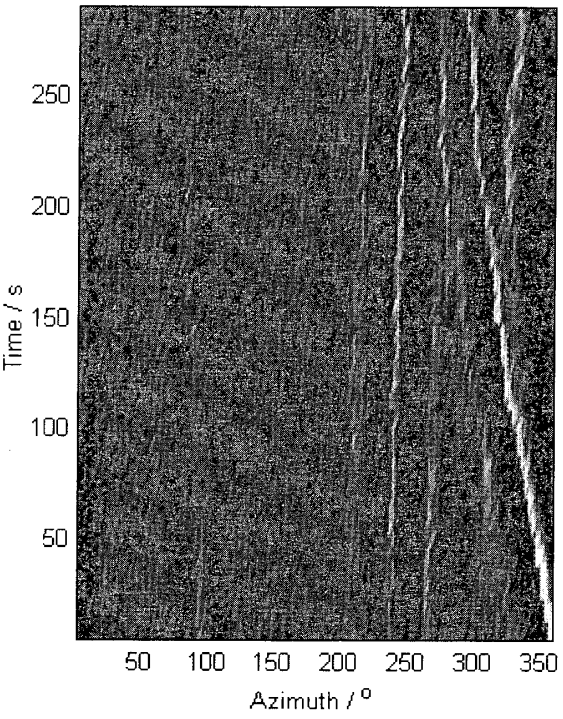

Fig. 8 BTR from SPED.

References

[1] B. D. Van Veen and K. M. Buckley, "Beamforming: A versatile approach to spatial filtering," *IEEE ASSP Mag.*, **5**, 4–24 (1988).
[2] R. O. Nielsen, *Sonar Signal Processing* (Interstate Electronics Corporation Anaheim, California, Artech House, Inc., 1991).
[3] R. F. Follett, "High resolution broadband FFT beamformer simulation and analysis," *Proc. Symp. Autonomous Underwater Vehicle Technology*, pp. 254–259 (1990).
[4] R. F. Follett and J. P. Donohoe, "A wideband, high-resolution, low-probability-of-detection FFT beamformer," *IEEE J. Ocean. Eng.*, **19**, 175–182 (1994).
[5] M. Bono, B. Shapo, P. McCarty and R. Bethel, "Subband energy detection in passive array processing," *Adaptive Sensor Array Processing (ASAP) Workshop*, MIT: LL, March, pp. 13–14 (2001).
[6] S.-F. Yan and Y.-L. Ma, "Broadband passive signal detection through hydrophone array optimization and SPED processing," *2nd China-Japan Jt. Conf. on Acoustics* (2002).
[7] B.-C. Kim and I.-T. Lu, "High resolution broadband beamforming based on the MVDR method," *OCEANS 2000 MTS/IEEE Conference and Exhibition*, Vol. 3, pp. 1673–1676 (2000).
[8] S. W. Davies and M. E. Knappe, "Noise background normalization for simultaneous broadband and narrowband detection," *Proc. ICASSP 88*, Vol. 5, pp. 2733–2736 (1988).
[9] T. Suojoki and I. Tabus, "A novel efficient normalization technique for sonar detection," *Proc. 2002 Int. Symp. Underwater Technology*, pp. 296–301 (2002).
[10] S. K. Mehta, J. Fay and P. Maciejewski, "A modified Eckart post-beamformer filter for improved detection using broadband features," *Proc. ICASSP 96*, pp. 3045–3048 (1996).